■ Metal-organic Frameworks │*Very Important Paper*│

ⱽᴵᴾ Solvent-Controlled Phase Transition of a Co^II-Organic Framework: From Achiral to Chiral and Two to Three Dimensions

Xing-Po Wang,[+][a] Wen-Miao Chen,[+][a] Hao Qi,[a] Xiao-Yi Li,[a] Cyril Rajnák,[b] Zhen-Yu Feng,[a] Mohamedally Kurmoo,*[c] Roman Boča,[b] Chun-Jiang Jia,[a] Chen-Ho Tung,[a] and Di Sun*[a]

Abstract: An unprecedented reversible dynamic transformation is reported in a metal-organic framework involving bond formation, which is accompanied by two important structural changes; achiral to chiral and two- to three-dimensions. Using two bent organic ligands (diimpym = 4,6-di(1H-imidazol-1-yl)pyrimidine; H_2npta = 5-nitroisophthalic acid) and $Co^{II}(NO_3)_2 \cdot 6H_2O$ the coordination polymer $Co(diimpym)(npta) \cdot CH_3OH$, (**1·CH₃OH**), was obtained solvothermally. Its structure consists of knitted pairs of square layers (4^4-**sql** net) of five-coordinated Co and disordered methanol, and it crystallized in the achiral *Pbca* space group at room temperature. It undergoes a single crystal to single crystal (SC-SC) transformation to a 3D interpenetrated framework (α-polonium-type net, **pcu**) of six-coordinated Co and ordered methanol in the chiral $P2_12_12_1$ space group below 220 K. Most unusual is the dynamic temperature-dependent shortening of a Co···O connection from a non-bonded 2.640 Å (298 K) to a bonded 2.347 Å distance (100 K) transforming the square pyramidal cobalt polyhedron to a distorted octahedron. The

desolvated crystals (**1**) obtained at 480 K retain the full crystallinity and crystallize in the achiral *Pbca* space group between 100 and 298 K but the dynamic shortening of the Co···O distance connecting the layers into the 3D **pcu** framework structure is observed. Following post-synthetic insertion of ethanol (**1·CH₃CH₂OH**) it does not exhibit the transformation and retains the knitted 2D achiral *Pbca* structure for all temperatures (100–298 K) and the ethanol is always disordered. The structural analyses thus conclude that the ordering of the methanol induces the chirality while the available space controls the dynamic motion of the knitted 2D networks into the 3D interpenetrated framework. Consequently, **1** selectively adsorbs CO_2 to N_2 and exhibits Type-III isotherms indicating dynamic motion of the 2D networks to accommodate the CO_2 at 273 and 298 K in contrast to the rigidity of the 3D framework at 77 K preventing N_2 from penetrating the solid. The magnetic properties are also reported.

[a] Dr. X.-P. Wang,[+] W.-M. Chen,[+] H. Qi, X.-Y. Li, Z.-Y. Feng, Prof. C.-J. Jia, Prof. C.-H. Tung, Dr. D. Sun
Key Lab of Colloid and Interface Chemistry
Ministry of Education
School of Chemistry and Chemical Engineering
Shandong University
Jinan, 250100 (P. R. China)
Fax: (+86) 531-88364218
E-mail: dsun@sdu.edu.cn

[b] Dr. C. Rajnák, Prof. R. Boča
Department of Chemistry, FPV
University of Ss. Cyril and Methodius
917 01 Trnava (Slovakia)

[c] Prof. M. Kurmoo
Institut de Chimie de Strasbourg
Université de Strasbourg, CNRS-UMR 7177
4 rue Blaise Pascal, 67008 Strasbourg Cedex (France)
E-mail: kurmoo@unistra.fr

[+] These authors contributed equally to this work.

▯ Supporting information including experimental and analytical details, and
ⓘ the ORCID identification number(s) for the author(s) of this article can be found under: http://dx.doi.org/10.1002/chem.201700474.

Introduction

Structural transformation from one crystalline phase to another without change of content of the unit cell is common in solid-state chemistry and the process is rather well understood thermodynamically.[1–2] Transformations involving changes of content in a single crystal to single crystal (SC-SC) manner have now been demonstrated in numerous cases both in situ and ex situ.[3–7] In general, the transformation is not a thermodynamic phase transition but a chemical process depending on the chemical entities and their electronic properties. As such the surface of the solid where the guests are incorporated is the active part that is concerned and therefore very relevant for catalytic reactions, storage of fuel gases, chromatographic separation, and control alignment of optical active components.[8–10]

The above mentioned transformations do not involve much movement of the connected atoms which are governed by the electronic characteristics of the atoms through covalent bonds for the organic moiety, coordination bonds around the metal centers, and weak supramolecular interactions are usually involved in the framework stability. The evolution from a very weak coordinate bond interaction to a much stronger coordi-

nate bond with retention of single crystal character is, to our knowledge, rare. Here, we present such a case in a coordination polymer, Co(diimpym)(npta)·CH$_3$OH (**1·CH$_3$OH**), obtained solvothermally using 4,6-di(1H-imidazol-1-yl)pyrimidine (diimpym), 5-nitroisophthalic acid (H$_2$npta) and Co^{II}(NO$_3$)$_2$·6H$_2$O. It consists of knitted square corrugated layers (4^4-**sql** net) of five-coordinated Co atoms and disordered methanol above 240 K. Below 240 K it is transformed into a 3D interpenetrated framework (α-polonium-type net, **pcu**) of six-coordinated Co and ordered methanol. The temperature dependent dynamic formation of a Co···O bond between the monomeric pyramidal Co (Co···O = 2.640 Å at 298 K) to a dimeric octahedral Co (Co···O = 2.347 Å at 100 K) is responsible for the structural transformation.

Given the very rare occurrence of crystals displaying achiral to chiral transformation from purely non-optically active components, the present case represents a unique case where the ordering of the methanol induces a reversible space group change from achiral *Pbca* above 240 K to chiral *P*2$_1$2$_1$2$_1$ below, without major changes of the lattice parameters. The desolvated form (**1**) that retains its crystallinity after removal of the methanol at 480 K, exhibits a 2D to 3D transformation as for **1·CH$_3$OH** but it retains the achiral *Pbca* structure. Following resolvation with ethanol, the **1·CH$_3$CH$_2$OH** crystals retain the 2D structure without transformation, space group change, and ordering of the ethanol.

These unique characteristics form the content of the present work through a thorough study of the single crystal to single crystal transformation in the temperature range 100 to 480 K. The different phases have been further characterized using TGA, IR, DSC, and diffuse reflectance UV/Vis spectroscopy. In addition we explore the selective gas sorption characteristics and their magnetic properties.

Results and Discussion

Crystal structure of [Co(diimpym)(npta)·CH$_3$OH]$_n$ (**1·CH$_3$OH**) at 298 K

The crystal structure of **1·CH$_3$OH** at 298 K adopts the orthorhombic centrosymmetric *Pbca* space group. The asymmetric unit contains one Co, one diimpym, one npta, and one disordered methanol molecule. The two organic ligands act as ditopic bridges through the peripheral nitrogen atoms of diimpym and the monodentate carboxylate oxygen atoms of npta. The central Co adopts a distorted square-pyramidal geometry ($\tau_5 = 0.32$)[11] with three O atoms from two npta and two N atoms from two diimpym (Co1−N = 2.035(3) and 2.084(3) Å; Co1−O = 1.986(2), 2.102(2), and 2.267(2) Å) (Figure 1a). The N1, O1, O3, and O4 build the basal square plane and the vertex position is occupied by N6. Another symmetry related O1^{iii} ($-x+2$, $-y+1$, $-z+1$) is *trans* to N6 but at a distance Co1···O1^{iii} of 2.640(2) Å, which is extremely long to be considered as a coordination bond. A Co^{II}−O bond length distribution analysis based on a CSD (Cambridge Structure Database) survey (Figure S1 in Supporting Information)[12] found >99% of Co−O distances fall between 1.8 and 2.3 Å, with only 5 examples longer than 2.4 Å. The diimpym has four potential co-
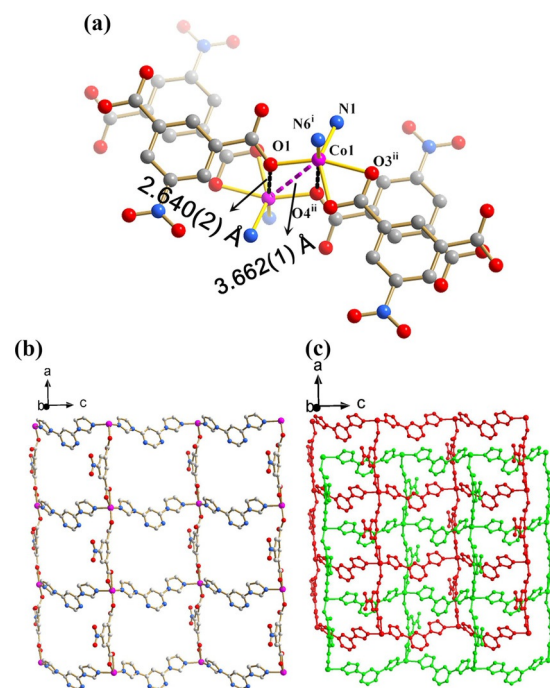

Figure 1. (a) The square-pyramidal coordination environment of Co^{II} in a pair of adjacent units of **1·CH$_3$OH** at 298 K with long Co1···O1^{iii} and Co···Co distances highlighted by black and purple dashed lines, respectively. Two separate nets are shown in depth cueing mode. (b) One 2D 4^4-**sql** network. (c) Two knitted 4^4-**sql** networks.

ordination sites but it only uses two N$_{imidazole}$ to bridge Co atoms into a zig-zag [Co(diimpym)]$_n$ chain running along the *c*-axis. The two carboxylate groups of npta adopt μ$_1$-κ^1:κ^1 and μ$_1$-κ^1:κ^0 coordination modes to extend the 1D zig-zag [Co(diimpym)]$_n$ chain into a 2D corrugated sheet (Figure 1b), which could be simplified to a 4^4-**sql** network with the size of rectangular window being 12.87 × 10.09 Å. Because of the large window sizes, two sheets are knitted with each other to form a 2D network (Figure 1c).

Crystal structure of [Co(diimpym)(npta)·CH$_3$OH]$_n$ (**1·CH$_3$OH**) at 100 K

In contrast, the crystal structure of **1·CH$_3$OH** at 100 K adopts the orthorhombic chiral *P*2$_1$2$_1$2$_1$ space group. The asymmetric unit is now doubled with two Co atoms, two diimpym and two ordered methanol molecules. The Co^{II} now has an additional coordination resulting in an octahedral geometry (three O and three N atoms). In this octahedral environment, there are two moderately long coordination bonds, Co1−O1^{ii} (2.395(3) Å) and Co2−O10^{v} (2.347(3) Å), indicating the Jahn–Teller effect. The coordination mode of diimpym is unaltered but the npta takes a μ$_3$-κ^1:κ^1:κ^2:κ^0 mode, which binds Co1 and Co2 to form a binuclear secondary build unit (SBU). The extended mixed bridges connect the binuclear Co SBU to form a 3D framework (Figure 2b) consisting of two interpenetrated frameworks (Figure 2c). The methanol molecules are now ordered and this is the reason for the lowering of symmetry and inducing the chirality. Considering the binuclear Co SBU as the
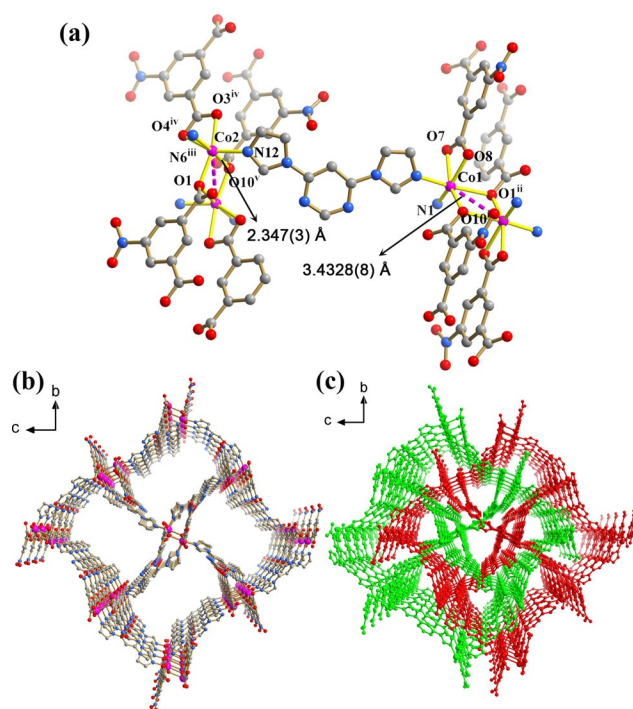
(a)

(b)

(c)

Figure 2. (a) The distorted octahedral coordination environment of Co^{II} in a pair of adjacent units of **1·CH$_3$OH** at 100 K with shortened Co···Co distances highlighted by purple dashed lines. (b) A 3D *pcu* network. (c) The 2-fold interpenetrated *pcu* networks (networks individually colored). Symmetry codes: (i) $x-1$, y, z; (ii) $-x+1$, $y-1/2$, $-z+3/2$; (iii) x, y, $z+1$; (iv) $x+1$, y, z; (v) $-x+2$, $y+1/2$, $-z+3/2$.

node and the ligand as 2-connected linker, the 3D framework could be simplified to a 6-connected *pcu* topology (Figure 2c) with a point symbol of $\{4^{12}.6^3\}$. The 2-fold interpenetration belongs to Class **IIa**; related to the crystallographic 2_1 axis. In the whole view, the 3D structure of **1·CH$_3$OH** at 100 K can be seen transformed from the addition of one new Co—O coordination bond between two pristine knitted corrugated layers at 298 K.

Temperature-induced phase transition for 1·CH$_3$OH

The crystal structures of **1·CH$_3$OH** at 280, 260, and 240 K, all in *Pbca* space group (Table S1 in Supporting Information), were found to be very similar to that at 298 K except for the slight contraction of the lattice and small changes in bond distances. The Co1···O1^{iii} and Co1···Co1^{ii} distances decrease noticeably from 2.640(2) and 3.6623(10) Å at 298 K to 2.500(5) and 3.5463(19) Å at 240 K, respectively (Figure 3 and Table S7). Upon further cooling from 240 to 220 K the lattice changes space group from centrosymmetric *Pbca* (Point group: mmm) to chiral $P2_12_12_1$ (Point group: 222) while the lattice parameters *a*, *b*, and *c* do not change significantly during the phase transition. However, the composition of the asymmetric unit is doubled and the lattice methanol molecules become ordered below 220 K. The Co1—O1^{ii} and Co2—O1^v distances (corresponding to Co1···O1^{iii} above 240 K) gradually shortened from 2.501(4) and 2.442(3) Å to 2.395(3) and 2.347(3) Å from 220 to 100 K. The shortened interatomic distances indicated the formation of a new coordination bond, which transforms the
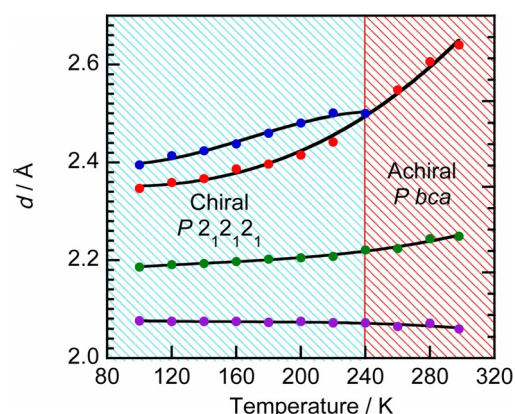

Figure 3. The temperature dependence of the bond distances: Co1—O1 (blue and red symbols) and the average Co—N (purple) and Co—O (green) bond lengths

single Co SBU to a binuclear Co SBU accompanying the change of the linkage mode of the ntpa ligand from μ_2-κ^1:κ^1:κ^1:κ^0 to μ_3-κ^1:κ^1:κ^2:κ^0 (Figure 4a and b). Consequently, the structure evolved from a knitted 4^4-*sql* layered network to a 3D 2-fold interpenetrated *pcu* framework.

The transformation involving the network dimensionality and space group changes can be mainly attributed to the dynamic formation of an additional Co—O coordination bond and the order-to-disorder of the methanol molecules in the lattice. It is a lesson to be learnt that it may be useful to determine the structure at low temperatures because certain details may be overlooked even though the unit-cell parameters often do not change dramatically, such as in this case.

Thermogravimetric analysis (Figure S2) indicates that the lattice CH$_3$OH molecules are completely lost by 453 K (obs. 6.08 %; calc. 6.25 %) and the framework of **1** is stable up to 635 K. When crystals of **1·CH$_3$OH** were heated at 480 K for 30 minutes, then subjected to X-ray diffraction, the crystallinity and structure of the desolvated **1** was as good as that of **1·CH$_3$OH**, confirming [Co(diimpym)(npta)]$_n$ undergoes a SC-SC transformation. One selected crystal was also examined by hot-stage microscopy and its morphology was monitored during heating from room temperature to 723 K. We found the morphology was kept intact even at 673 K, which also supported its high stability at high temperature (Figure S3). The structure of **1** adopts the same space group (*Pbca*) and overall connectivity of the network as that of **1·CH$_3$OH** at 298 K. The absence of the methanol generates channels of similar geometry and dimensions (Figure 4c). Even though **1·CH$_3$OH** and **1** are 2D networks at high temperature, it is indeed surprising that the structure is stable to the removal of methanol. Often low dimensional porous MOFs lose their crystallinity after guest removal at high temperatures, unlike the SC-SC transformation of **1·CH$_3$OH**.

Selective guest inclusion and phase switching process

Because of the permanent porosity of **1**, found by single-crystal diffraction analyses, we studied the inclusion behaviors of **1** toward different guest molecules: H$_2$O, CH$_3$OH, CH$_3$CN,
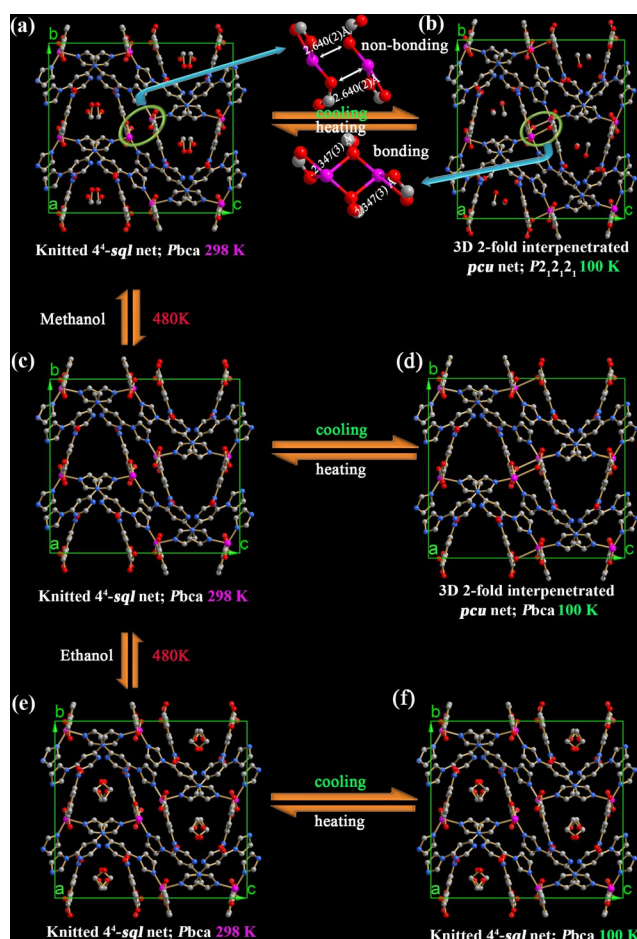
Figure 4. Representation of the reversible transformation of **1·CH₃OH** from (a) knitted 4^4-*sql* network at 298 K to (b) 3D 2-fold interpenetrated *pcu* framework at 100 K. The characteristic Co—O non-bonding or bonding was highlighted above and below the arrows. (c) The desolvated phase **1** produced by heating at 480 K and (d) the 3D interpenetrated structure of **1** formed by cooling to 100 K. (e) The ethanol inclusion induced SC-SC transformation from desolvated phase **1** with no noticeable structural changes observed when cooling to 100 K (f).

C_2H_5OH, *n*-propanol, *iso*-propanol, *n*-butanol, and glycol, at room temperature. When immersing crystals of **1** into H_2O,

CH_3OH, *n*-propanol, *iso*-propanol, *n*-butanol, and glycol their appearance and crystal habits were maintained in contrast to the breaking of the rod-like crystals into small pieces when immersed in CH_3CN and C_2H_5OH. In the case of C_2H_5OH the broken crystals still diffract and their structure was determined at 298 and 100 K. It revealed the same knitted 2D layers (space group *Pbca*) as for **1·CH₃OH** at 298 K, with a disordered ethanol molecule at both temperatures. The transformation to the 3D 2-fold interpenetrated *pcu* framework (as found for **1·CH₃OH** at 100 K) is prevented by the steric effect of the large ethanol and its disordered state (Figure 4 d). Although the CH_3CH_2OH molecules in the channels are still disordered at 100 K the anisotropic displacement parameters are lowered with respect to those at 298 K. This finding demonstrates that the dynamics can be controlled by the available space.

When crystals of **1·CH₃OH** are heated at 480 K the methanol molecules are released to form **1**. Its structure after cooling to 100 K at a rate of 5 K min⁻¹ adopts the $P2_12_12_1$ space group (Table 1) with the 3D 2-fold interpenetrated *pcu* framework. A summary of the space group and network dimensionality as well as schematic graphics are given in Table 2. By comparing the coordination networks of **1·CH₃OH**, **1**, and **1·CH₃CH₂OH** and the guest molecule status, we found the change of space group is driven by the order-to-disorder transformation of methanol molecules within the channels, while the presence of free space allows for dynamic motion of the adjacent 2D knitted networks to connect into the 3D interpenetrated framework. Thus, the existence of a temperature-dependent order-to-disorder transformation of solvents alters the crystallographic symmetry, changing the space group to a chiral one.

Magnetic properties of 1, 1·CH₃OH, and 1·CH₃CH₂OH

The magnetic data were measured using powder samples on a SQUID-MPMS3 magnetometer (Quantum Design). The susceptibility data (1 kOe) were corrected for the underlying diamagnetism. The temperature dependence of the effective magnetic moment, and the field dependence of the magnetization per formula unit are presented in Figure 5 for **1** and Fig-

Table 1. Summary of crystallographic data for **1·CH₃OH**, **1**, and **1·CH₃CH₂OH** at 100 and 298 K.

Compound	1·CH₃OH		1		1·CH₃CH₂OH	
T [K]	100	298	100	298	100	298
crystal system	orthorhombic	orthorhombic	orthorhombic	orthorhombic	orthorhombic	orthorhombic
space group	$P2_12_12_1$	*Pbca*	*Pbca*	*Pbca*	*Pbca*	*Pbca*
a [Å]	10.0389(16)	10.088(2)	10.1365(11)	10.1211(11)	10.087(3)	10.093(6)
b [Å]	19.730(3)	19.229(4)	19.047(2)	19.240(2)	19.268(6)	19.074(12)
c [Å]	20.131(3)	20.815(4)	20.586(2)	20.891(2)	20.930(6)	21.537(13)
V [Å³]	3987.3(11)	4037.7(15)	3974.5(7)	4068.2(7)	4068(2)	4146(4)
reflections collected	19070	18076	18806	24437	13007	11118
independent reflections	8798	4627	3495	3562	3544	3628
R_{int}	0.0518	0.1543	0.0254	0.0571	0.0867	0.1606
data/parameters	8798/616	4627/301	3495/289	3562/289	3544/0/325	3628/3/306
GOF	0.993	0.795	1.032	1.090	1.038	1.023
R_1 [I > 2σ (I)][a]	0.0472	0.0458	0.0272	0.0545	0.0537,	0.0931
wR_2 [I > 2σ (I)][a]	0.0926	0.0988	0.0772	0.1482	0.1171	0.1891

[a] $R_1 = \Sigma ||F_o| - |F_c|| / \Sigma |F_o|$, $wR_2 = [\Sigma w (F_o^2 - F_c^2)^2 / \Sigma w (F_o^2)^2]^{1/2}$.

Table 2. Summary of space group and network phase transition.

	1·CH$_3$OH		1		1·CH$_3$CH$_2$OH	
temperature [K]	298	100	298	100	298	100
space group	Pbca	P2$_1$2$_1$2$_1$	Pbca	Pbca	Pbca	Pbca
dimensionality	2D[a]	3D[b]	2D[a]	3D[b]	2D[a]	2D[a]
structural node	monomer	dimer	monomer	dimer	monomer	monomer
solvent molecule	disordered	ordered	N/A	N/A	disordered	disordered
schematic representation of the phase transition						

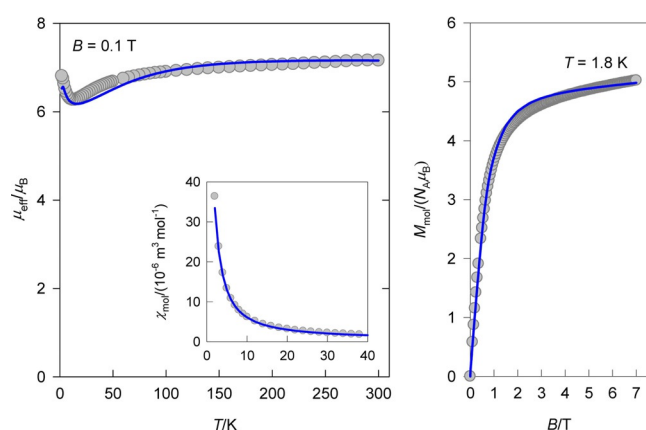[a] Knitted 4^4-*sql* network; [b] 2-fold interpenetrated *pcu* framework.

Figure 5. DC magnetic data for **1**: (left) temperature dependence of the effective magnetic moment per cobalt ion (inset: temperature dependence of the molar magnetic susceptibility); (right) field dependence of the magnetization (Blue solid lines are fits; see text for details).

ures S6–S7 in Supporting Information for **1·CH$_3$OH** and **1·CH$_3$CH$_2$OH**.

The effective magnetic moment at the room temperature is $\mu_{eff} = 4.90\ \mu_B$ which is within the experimentally observed range for Co^{II} complexes. On cooling, the effective magnetic moment is almost constant down to $T \approx 100$ K. Below this temperature a gradual decrease is registered that is caused by a considerable single ion anisotropy measured by the axial zero-field splitting parameter D. Below 20 K, however, an increase of μ_{eff} is registered due the exchange coupling of a ferromagnetic nature. The magnetization per cobalt ion deviates from the hypothetical limit of $M_{mol}/N_A = 3.0\ \mu_B$ for $S = 3/2$ centers with $g = 2.0$ and at $T = 1.8$ K it shows a value of only $2.35\ \mu_B$. This is a fingerprint of a sizable zero-field splitting. There is no anomaly that can be associated with the phase transitions suggesting the interaction between nearest neighbor cobalt is weak.

The crystal structure of the system under study is too complex in order to apply a complete model for exchange coupling incorporating a single-ion anisotropy. The magnetic data was therefore fitted using a model of the exchange-coupled pair with zero-field splitting (see Supporting Information). The

fitting procedure converged to the following set of magnetic parameters for **1**: $J/hc = 1.44$ cm^{-1}, $g_{av} = 2.62$, $D/hc = 83.3$ cm^{-1}. These values span ranges typical for hexacoordinate Co^{II} complexes.[13] The magnetic data for **1·CH$_3$OH** and **1·CH$_3$CH$_2$OH** exhibit a similar behavior to **1**. Thus the incorporation of the solvent molecules into the crystal lattice does not alter the overall magnetic behavior, although the solvents are involved in the phase transition. There is no noticeable change in the magnetization at the structural transition.

Selective gas sorption

When the methanol in **1·CH$_3$OH** is removed, channels of **1** are generated by the interconnection of irregular cavities running along the *a*-axis. The 1D channel has a trigonal window with maximum radius of 1.70 Å, that is, a maximum diameter of 3.40 Å. The total solvent-accessible volume of 12.0 % is estimated using PLATON. The robust porous network of **1** and the exposed Lewis basic sites at the pyrimidyl group encouraged us to study the gas adsorption and separation properties toward CO$_2$ and N$_2$. Initially, the methanol of **1·CH$_3$OH** is removed at 393 K under the high vacuum for 2 h to get **1**. The variable temperature PXRD patterns matched well with those simulated from X-ray data, again confirming that **1** has almost identical structure as that of the host framework of **1·CH$_3$OH** (Figure S8 in Supporting Information). The sorption isotherms for N$_2$ and CO$_2$ are shown in Figure 6a. The isotherms for CO$_2$ behave as reversible Type-III, suggesting the retention of the microporous structure after removal of the guest molecules. At 77 K, negligible N$_2$ sorption was observed; whereas the adsorption curve for CO$_2$ shows a rapid increase with pressure and reaches the maximum uptake capacities of 34.3 and 18.9 cm^{3}g^{-1} at 273 and 295 K, respectively. These results demonstrate the selective adsorption of CO$_2$ over N$_2$, although the CO$_2$ uptake capacities are inferior to some reported materials.[14] It is also noteworthy that the CO$_2$ adsorption–desorption cycle at 273 K exhibits hysteresis, which could be associated with interaction of CO$_2$ with the network (see above). In order to obtain more insight into the interaction of the adsorbate with the network, the isosteric heat (Q_{st}) of CO$_2$ was calculated by fitting the CO$_2$ adsorption isotherms at 273 and 295 K and has the estimated value of
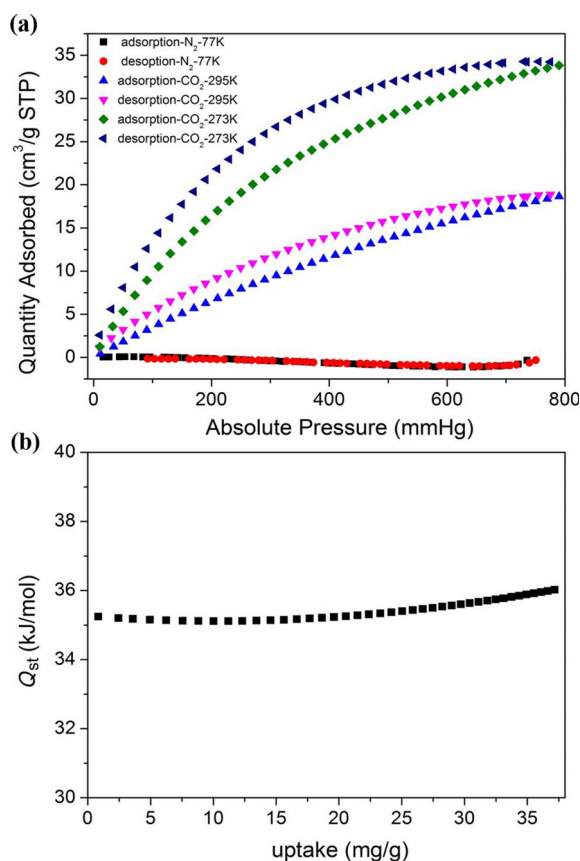
Figure 6. (a) CO_2 (273 and 298 K) and N_2 (77 K) adsorption capacity for **1**. (b) The Q_{st} of **1** for CO_2.

ethanol prevents the motion of the two dimensional knitted layers. The results warn us to be more cautious with concluding no change to structure when the lattice parameters and PXRD are retained. A Type-III CO_2 adsorption isotherm is observed at 298 K and N_2 is not incorporated in the pores at 77 K, suggesting motion of the knitted layers to accommodate the CO_2 while the 3D framework is too rigid, preventing N_2 sorption. Such dynamic structural motion can be very useful in chromatography and separation by accommodating molecules larger than available pore sizes. The material can be also used to adsorb gases at high temperature and to release them by cooling due to the bond formation induced by contraction.

Conflict of interest

The authors declare no conflict of interest.

Keywords: gas adsorption · magnetism · metal-organic frameworks · single-crystal-to-single-crystal transformation

36 kJ mol^{-1}, which suggests moderate interactions (Figure 6 b).[15] However, the enthalpy of adsorption is smaller than that observed in typical chemical adsorption. Thus, the interaction within **1** is primarily a physical adsorption in nature. On the basis of the obtained results, we reasoned that the selective adsorption behavior of **1** should be assigned to i) the presence of the exposed pyrimidyl moieties and ii) the accessibility of electron rich organic ligands, which creates the a polar pore wall that preferentially adsorbs CO_2 because of its high quadrupole moment and polarizability.[16]

Conclusion

In summary, two very unique unprecedented characteristics of the present metal-organic framework have been evidenced in this study. One is the phenomenal dynamic transformation of knitted square layers into a three-dimensional framework induced by an unusual coordinate bond shortening between neighboring monomeric (Co⋯O = 2.640 Å) units to dimers (Co⋯O = 2.347 Å). This happens without any abrupt change to the lattice parameters and powder X-Ray diffraction patterns. The second is the ordering of methanol solvent inducing a change of space group from achiral *Pbca* at high temperature to chiral *P*2$_1$2$_1$2$_1$ at low temperature. While removal of the methanol results in the retention of the achiral space group *Pbca* between 100 and 480 K, its replacement by the larger

[1] a) H. Furukawa, K. E. Cordova, M. O'Keeffe, O. M. Yaghi, *Science* **2013**, *341*, 1230444; b) X.-Z. Song, S.-Y. Song, S.-N. Zhao, Z.-M. Hao, X. Zhu, X. Meng, L.-L. Wu, H.-J. Zhang, *Adv Funct Mater.* **2014**, *24*, 4034; c) J. M. Falkowski, C. Wang, S. Liu, W. Lin, *Angew. Chem. Int. Ed.* **2011**, *50*, 8674; *Angew. Chem.* **2011**, *123*, 8833; d) Y.-G. Huang, B. Mu, P. M. Schoenecker, C. G. Carson, J. R. Karra, Y. Cai, K. S. Walton, *Angew. Chem. Int. Ed.* **2011**, *50*, 436; *Angew. Chem.* **2011**, *123*, 456; e) X. Li, H. Xu, F. Kong, R. Wang, *Angew. Chem. Int. Ed.* **2013**, *52*, 13769; *Angew. Chem.* **2013**, *125*, 14014; f) L. Ma, C.-D. Wu, M. M. Wanderley, W. Lin, *Angew. Chem. Int. Ed.* **2010**, *49*, 8244; *Angew. Chem.* **2010**, *122*, 8420; g) C. D. Wu, W. B. Lin, *Angew. Chem. Int. Ed.* **2005**, *44*, 1958; *Angew. Chem.* **2005**, *117*, 1994; h) Y.-C. He, J. Yang, G.-C. Yang, W.-Q. Kan, J.-F. Ma, *Chem. Commun.* **2012**, *48*, 7859; i) Q.-K. Liu, J.-P. Ma, Y.-B. Dong, *Chem. Commun.* **2011**, *47*, 12343; j) A. Michaelides, S. Skoulika, M. G. Siskos, *Chem. Commun.* **2011**, *47*, 7140; k) H.-R. Fu, Z.-X. Xu, J. Zhang, *Chem. Mater.* **2015**, *27*, 205; l) C. Wang, L. Li, J. G. Bell, X. Lv, S. Tang, X. Zhao, K. M. Thomas, *Chem. Mater.* **2015**, *27*, 1502; m) J. Tian, L. V. Saraf, B. Schwenzer, S. M. Taylor, E. K. Brechin, J. Liu, S. J. Dalgarno, P. K. Thallapally, *J. Am. Chem. Soc.* **2012**, *134*, 9581; n) M. C. Bernini, F. Gandara, M. Iglesias, SN. nejko, E. Gutierrez-Puebla, E. V. Brusau, G. E. Narda, M. A. Monge, *Chem-Eur. J.* **2009**, *15*, 4896; o) M. C. Das, P. K. Bharadwaj, *Chem-Eur. J.* **2010**, *16*, 5070.

[2] a) M.-H. Xie, X.-L. Yang, C.-D. Wu, *Chem-Eur. J.* **2011**, *17*, 11424; b) A. Aijaz, P. Lama, P. K. Bharadwaj, *Inorg. Chem.* **2010**, *49*, 5883; c) S. Bhattacharya, A. J. Bhattacharyya, S. Natarajan, *Inorg. Chem.* **2015**, *54*, 1254; d) Y.-P. Cai, X.-X. Zhou, Z.-Y. Zhou, S.-Z. Zhu, P. K. Thallapally, J. Liu, *Inorg. Chem.* **2009**, *48*, 6341; e) J.-P. Zhao, B.-W. Hu, Q. Yang, T.-L. Hu, X.-H. Bu, *Inorg. Chem.* **2009**, *48*, 7111; f) R. J. Wei, Q. Huo, J. Tao, R. B. Huang, L. S. Zheng, *Angew. Chem. Int. Ed.* **2011**, *50*, 8940; *Angew. Chem.* **2011**, *123*, 9102; g) B. Li, R.-J. Wei, J. Tao, R.-B. Huang, L.-S. Zheng, Z. Zheng, *J. Am. Chem. Soc.* **2010**, *132*, 1558; h) D. K. Smith, *Chem. Soc. Rev.* **2009**, *38*,

684–694; i) J. Han, S. Nishihara, K. Inoue, M. Kurmoo, *Inorg. Chem.* **2014**, *53*, 2068.

[3] a) T. N. Hoheisel, S. Schrettl, R. Marty, T. K. Todorova, C. Corminboeuf, A. Sienkiewicz, R. Scopelliti, W. B. Schweizer, H. Frauenrath, *Nat. Chem.* **2013**, *5*, 327; b) P. Kissel, D. J. Murray, W. J. Wulftange, V. J. Catalano, B. T. King, *Nat. Chem.* **2014**, *6*, 774; c) D. Liu, J.-P. Lang, B. F. Abrahams, *J. Am. Chem. Soc.* **2011**, *133*, 11042; d) M. Garai, R. Santra, K. Biradha, *Angew. Chem. Int. Ed.* **2013**, *52*, 5548; *Angew. Chem.* **2013**, *125*, 5658; e) G. K. Kole, T. Kojima, M. Kawano, J. J. Vittal, *Angew. Chem. Int. Ed.* **2014**, *53*, 2143; *Angew. Chem.* **2014**, *126*, 2175; f) D. Liu, Z.-G. Ren, H.-X. Li, J.-P. Lang, N.-Y. Li, B. F. Abrahams, *Angew. Chem. Int. Ed.* **2010**, *49*, 4767; *Angew. Chem.* **2010**, *122*, 4877; g) K. Tanaka, F. Toda, E. Mochizuki, N. Yasui, Y. Kai, I. Miyahara, K. Hirotsu, *Angew. Chem. Int. Ed.* **1999**, *38*, 3523; *Angew. Chem.* **1999**, *111*, 3733; h) N. L. Toh, M. Nagarathinam, J. J. Vittal, *Angew. Chem. Int. Ed.* **2005**, *44*, 2237; *Angew. Chem.* **2005**, *117*, 2277; i) M. R. Warren, S. K. Brayshaw, A. L. Johnson, S. Schiffers, P. R. Raithby, T. L. Easun, M. W. George, J. E. Warren, S. J. Teat, *Angew. Chem. Int. Ed.* **2009**, *48*, 5711; *Angew. Chem.* **2009**, *121*, 5821; j) S. Dutta, D.-K. Bucar, E. Elacqua, L. R. MacGillivray, *Chem. Commun.* **2013**, *49*, 1064; k) Y.-F. Han, Y.-J. Lin, W.-G. Jia, G.-L. Wang, G.-X. Jin, *Chem. Commun.* **2008**, 1807.

[4] a) E. Y. Lee, M. P. Suh, *Angew. Chem. Int. Ed.* **2004**, *43*, 2798; *Angew. Chem.* **2004**, *116*, 2858; b) M. H. Mir, L. L. Koh, G. K. Tan, J. J. Vittal, *Angew. Chem. Int. Ed.* **2010**, *49*, 390; *Angew. Chem.* **2010**, *122*, 400; c) D.-m. Chen, W. Shi, P. Cheng, *Chem. Commun.* **2015**, *51*, 370; d) S. Yuan, Y.-K. Deng, D. Sun, *Chem-Eur. J.* **2014**, *20*, 10093; e) T. Zheng, J. M. Clemente-Juan, J. Ma, L. Dong, S.-S. Bao, J. Huang, E. Coronado, L.-M. Zheng, *Chem-Eur. J.* **2013**, *19*, 16394; f) C.-F. Zhuang, J. Zhang, Q. Wang, Z.-H. Chu, D. Fenske, C.-Y. Su, *Chem-Eur. J.* **2009**, *15*, 7578; g) S. Bhattacharya, A. J. Bhattacharyya, S. Natarajan, *Inorg. Chem.* **2015**, *54*, 1254; h) H. J. Choi, M. P. Suh, *J. Am. Chem. Soc.* **2004**, *126*, 15844; i) Q.-K. Liu, J.-P. Ma, Y.-B. Dong, *J. Am. Chem. Soc.* **2010**, *132*, 7005.

[5] a) A. S. Filatov, O. Hietsoi, Y. Sevryugina, N. N. Gerasimchuk, M. A. Petrukhina, *Inorg. Chem.* **2010**, *49*, 1626; b) R. Gheorghe, M. Kalisz, R. Clérac, C. Mathoniere, P. Herson, Y. Li, M. Seuleiman, R. Lescouëzec, F. Lloret, M. Julve, *Inorg Chem.* **2010**, *49*, 11045; c) J. P. Zhang, Y. Y. Lin, W. X. Zhang, X. M. Chen, *J. Am. Chem. Soc.* **2005**, *127*, 14162; d) T. Pretsch, K. W. Chapman, G. J. Halder, C. J. Kepert, *Chem. Commun.* **2006**, 1857; e) X.-F. Wang, Y. Wang, Y.-B. Zhang, W. Xue, J.-P. Zhang, X.-M. Chen, *Chem. Commun.* **2012**, *48*, 133.

[6] a) T. Seki, K. Sakurada, H. Ito, *Angew. Chem. Int. Ed.* **2013**, *52*, 12828; *Angew. Chem.* **2013**, *125*, 13062; b) J. Sun, F. Dai, W. Yuan, W. Bi, X. Zhao, W. Sun, D. Sun, *Angew. Chem. Int. Ed.* **2011**, *50*, 7061; *Angew. Chem.* **2011**, *123*, 7199; c) Y.-J. Zhang, T. Liu, S. Kanegawa, O. Sato, *J. Am. Chem. Soc. J. Am. Chem. Soc.*. **2009**, *131*, 7942–7943; d) J. Zhou, G.-Q. Bian, J. Dai, Y. Zhang, A.-b. Tang, Q.-Y. Zhu, *Inorg. Chem.* **2007**, *46*, 1541; e) L.-H. Cao, Y.-S. Wei, H. Xu, S.-Q. Zang, T. C. W. Mak, *Adv Funct Mater* **2015**, *25*, 6448–6457; f) X. Y. Dong, B. Li, B. B. Ma, S. J. Li, M. M. Dong, Y. Y. Zhu, S. Q. Zang, Y. Song, H. W. Hou, T. C. W. Mak, *J. Am. Chem. Soc.* **2013**, *135*, 10214–10217; g) R.-W. Huang, Y.-S. Wei, X.-Y. Dong, X.-H. Wu, C.-X. Du, S.-Q. Zang, T. C. W. Mak, *Nat Chem.* **2017**, 10.1038/nchem.2718.

[7] a) T.-F. Liu, L. Zou, D. Feng, Y.-P. Chen, S. Fordham, X. Wang, Y. Liu, H.-C. Zhou, *J. Am. Chem. Soc.* **2014**, *136*, 7813; b) T. Haneda, M. Kawano, T. Kawamichi, M. Fujita, *J. Am. Chem. Soc.* **2008**, *130*, 1578; c) G. Mukherjee, K. Biradha, *Chem. Commun.* **2012**, *48*, 4293; d) J. Li, P. Huang, X.-R. Wu, J. Tao, R.-B. Huang, L.-S. Zheng, *Chem. Sci.* **2013**, *4*, 3232; e) A. Bajpai, P. Chandrasekhar, S. Govardhan, R. Banerjee, J. N. Moorthy, *Chem-Eur. J.* **2015**, *21*, 2759.

[8] a) Z. Niu, J.-G. Ma, W. Shi, P. Cheng, *Chem. Commun.* **2014**, *50*, 1839; b) Y.-C. Ou, W.-T. Liu, J.-Y. Li, G.-G. Zhang, J. Wang, M.-L. Tong, *Chem. Commun.* **2011**, *47*, 9384; c) A. M. Fracaroli, P. Siman, D. A. Nagib, M. Suzuki, H. Furukawa, F. D. Toste, O. M. Yaghi, *J. Am. Chem. Soc.* **2016**, *138*, 8352.

[9] a) D. Liu, T.-F. Liu, Y.-P. Chen, L. Zou, D. Feng, K. Wang, Q. Zhang, S. Yuan, C. Zhong, H.-C. Zhou, *J. Am. Chem. Soc.* **2015**, *137*, 7740; b) H. Liu, C.-Y. Song, R.-W. Huang, Y. Zhang, H. Xu, M.-J. Li, S.-Q. Zang, G.-G. Gao, *Angew. Chem. Int. Ed.* **2016**, *55*, 3699; *Angew. Chem.* **2016**, *128*, 3763.

[10] a) Y. Abe, S. Karasawa, N. Koga, *Chem-Eur. J.* **2012**, *18*, 15038; b) Q.-Q. Li, C.-Y. Ren, Y.-Y. Huang, J.-L. Li, P. Liu, B. Liu, Y. Liu, Y.-Y. Wang, *Chem-Eur. J.* **2015**, *21*, 4703; c) H. J. Park, M. P. Suh, *Chem-Eur. J.* **2008**, *14*, 8812; d) Z. Yin, Q.-X. Wang, M.-H. Zeng, *J. Am. Chem. Soc.* **2012**, *134*, 4857; e) M.-H. Zeng, Q.-X. Wang, Y.-X. Tan, S. Hu, H.-X. Zhao, L.-S. Long, M. Kurmoo, *J. Am. Chem. Soc.* **2010**, *132*, 2561; f) M.-H. Zeng, Y.-X. Tan, Y.-P. He, Z. Yin, Q. Chen, M. Kurmoo, *Inorg. Chem.* **2013**, *52*, 2353; g) R. Sen, D. Saha, S. Koner, P. Brandao, Z. Lin, *Chem. Eur. J.* **2015**, *21*, 5962; i) T. Seki, K. Sakurada, M. Muromoto, H. Ito, *Chem. Sci.* **2015**, *6*, 1491.

[11] A. W. Addison, T. N. Rao, J. Reedijk, J. Van Rijn, G. C. Verschoor, *J. Chem. Soc. Dalton Trans.* **1984**, 1349.

[12] a) F. H. Allen, *Acta Crystallogr. Sect. A* **2002**, *58*, 380; b) Cambridge Structure Database search, CSD Version 5.28 November 2006 (with 25 updates January 2007-May 2013).

[13] a) Y. Z. Zheng, G. J. Zhou, Z. P. Zheng, R. E. P. Winpenny, *Chem. Soc. Rev.* **2014**, *43*, 1462; b) C. Rajnák, J. Titiš, O. Fuhr, M. Ruben, R. Boča, *Inorg. Chem.* **2014**, *53*, 8200.

[14] a) T. M. McDonald, D. M. D'Alessandro, R. Krishna, J. R. Long, *Chem. Sci.* **2011**, *2*, 2022; b) S. Chen, J. Zhang, T. Wu, P. Feng, X. Bu, *J. Am. Chem. Soc.* **2009**, *131*, 16027.

[15] a) B. Zheng, J. Bai, J. Duan, L. Wojtas, M. J. Zaworotko, *J. Am. Chem. Soc.* **2011**, *133*, 748; b) L. Mathivathanan, J. Torres-King, J. N. Primera-Pedrozo, O. J. Garcia-Ricard, A. J. Hernandez-Maldonado, J. A. Santana, R. G. Raptis, *Cryst. Growth Des.* **2013**, *13*, 2628.

[16] a) R. Vaidhyanathan, S. S. Iremonger, G. K. H. Shimizu, P. G. Boyd, S. Alavi, T. K. Woo, *Science* **2010**, *330*, 650; b) J. R. Li, R. J. Kuppler, H. C. Zhou, *Chem. Soc. Rev.* **2009**, *38*, 1477.